

*PIEZOMAGNETISM IN THE ANTIFERROMAGNETIC FLUORIDES OF COBALT AND  
MANGANESE*

A. S. BOROVIK-ROMANOV

Institute of Physical Problems, Academy of Sciences, U.S.S.R.

Submitted to JETP editor November 6, 1959

J. Exptl. Theoret. Phys. (U.S.S.R.) **38**, 1088-1098 (April, 1960)

A special magnetic balance and press were constructed to observe piezomagnetism experimentally. In agreement with theoretical predictions, piezomagnetic moments  $m_7^D$  were found to appear in  $\text{CoF}_2$  and  $\text{MnF}_2$  on applying shear stresses  $\sigma_{ik}$ . The values of the piezomagnetic modulus are  $\sim 10^{-3}$  gauss  $(\text{kg}/\text{cm}^2)^{-1}$  for  $\text{CoF}_2$  and  $10^{-5}$  gauss  $(\text{kg}/\text{cm}^2)^{-1}$  for  $\text{MnF}_2$ . A detailed analysis of the results obtained is made in terms of the thermodynamic theory. Together with the piezomagnetic moment perpendicular to the direction of sublattice magnetization, which is equivalent to the well-studied weak transverse ferromagnetism, a moment was observed parallel to the sublattice magnetization, which is equivalent to a weak longitudinal ferromagnetism not previously observed.

## 1. INTRODUCTION

THE possibility in principle of a piezomagnetic effect has long been discussed. As early as 1928, Voigt<sup>1</sup> considered all the crystallographic classes in which, according to his view, a piezomagnetic effect was possible from symmetry considerations, i.e., the appearance of a spontaneous magnetic moment on applying elastic stresses. However, his treatment was erroneous, since he did not take into account the additional symmetry element,  $R$ , for magnetic crystals, which involves a change of sign of the magnetic moments on inversion.<sup>2</sup> The symmetry group of any paramagnetic crystal contains the transformation  $R$ , and therefore the appearance of a spontaneous moment different from zero is impossible here. In substances possessing magnetic structure (ferromagnets and antiferromagnets), the transformation  $R$ , enters only in combination with other symmetry elements; it follows that in principle such substances can be piezomagnetic.<sup>3,4</sup> Naturally, the greatest interest lies in the study of the piezomagnetic effect in antiferromagnets, which do not under normal conditions possess macroscopic spontaneous moments. Dzyaloshinskii,<sup>5</sup> from considerations of magnetic symmetry, indicated a number of actual antiferromagnets in which the piezomagnetic effect should be observed. More recently, Tavger<sup>6</sup> and Le Corre<sup>7</sup> determined the piezomagnetic tensors for antiferromagnets of all magnetic structure classes.

The piezomagnetic effect in antiferromagnets is closely connected with the appearance of weak ferromagnetism, which has been experimentally

studied in detail in  $\alpha\text{-Fe}_2\text{O}_3$ ,<sup>8</sup> and  $\text{MnCO}_3$  and  $\text{CoCO}_3$ .<sup>9,10</sup> A theoretical consideration of these phenomena<sup>11,12</sup> showed that in many cases, in the same crystallographic structure, different types of antiferromagnetic ordering with different magnetic symmetries are possible. Thus, magnetic symmetry in some types does not permit a spontaneous ferromagnetic moment, whilst in other types antiferromagnetism is accompanied by weak ferromagnetism. It follows that if, on the application of stress to a crystal not possessing a spontaneous moment, the crystal deforms in such a way that its magnetic symmetry changes, then a ferromagnetic moment can arise in it.

We have already communicated the discovery of the piezomagnetic effect in the fluorides of cobalt and manganese.<sup>13</sup> These compounds transform into the antiferromagnetic state in a temperature region convenient for study:  $\text{MnF}_2$  at  $T_N = 66.5^\circ\text{K}$ ,<sup>14</sup>  $\text{CoF}_2$  at  $T_N = 37.7^\circ\text{K}$ .<sup>15</sup> So, even at  $20^\circ\text{K}$ , the magnetization of the sub-lattices in them is almost saturated. Both substances have a simple tetragonal lattice (group  $D_{4h}^{14}$ ).<sup>16</sup> In the antiferromagnetic state the spins of the ions at the centers of the crystallographic cells are antiparallel to the spins of the ions at the corners of the cells<sup>17</sup> — as shown in Fig. 1. Dzyaloshinskii has shown<sup>5,18</sup> that in these compounds a piezomagnetic moment should be observed along all three axes,\*

\*In Dzyaloshinskii paper<sup>5</sup> a term was omitted in the expression for the thermodynamic potential responsible for the appearance of a piezo-magnetic moment along the  $z$  axis. A complete analysis of this problem was given in his dissertation.<sup>18</sup>

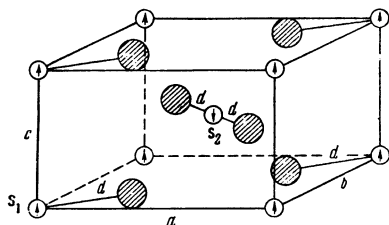


FIG. 1. The magnetic structure of  $MnF_2$  and  $CoF_2$ . Open circles - Mn, Co; shaded circles - F.

but only on applying shear stresses

$$m_x^p = \Lambda_1 \sigma_{yz}, \quad m_y^p = \Lambda_1 \sigma_{xz}, \quad m_z^p = \Lambda_2 \sigma_{xy}. \quad (1)$$

In a previous paper<sup>13</sup> we described the discovery of the "transverse" piezomagnetic moment ( $\Lambda_1 \sigma_{xz}$ ). In the present paper a more detailed description is given of the results of these experiments, and experiments demonstrating the "longitudinal" piezomagnetic moment ( $\Lambda_2 \sigma_{xy}$ ).

2. APPARATUS AND SPECIMENS

Considering the smallness of the expected piezomagnetic effect, we decided on the balance method of measuring magnetic moments as the most sensitive of known methods. A diagram of the apparatus we used is shown in Fig. 2. The specimen under study, 1, situated in tube 2 of press 3, lay in the inhomogeneous field of the electromagnet 4, 5.

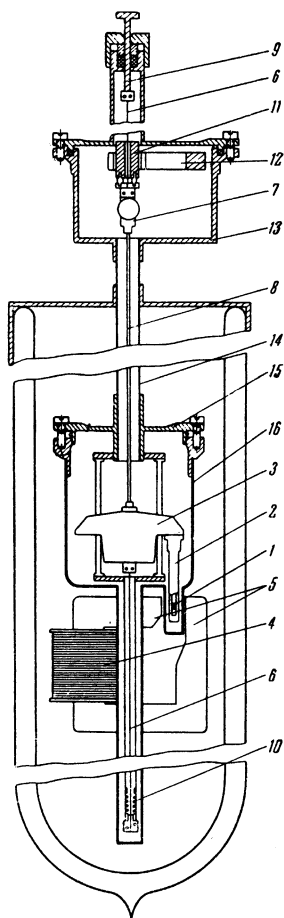


FIG. 2. Diagram of the magnetic torsion balance.

The use of a small electromagnet situated directly inside the Dewar excluded all effects involving the magnetization of the material from which the press was made.

If the specimen possesses a magnetic moment  $m$ , then the force

$$F_z = CmH,$$

acts on it, where the constant  $C = H^{-1} dH/dz$  depends on the position of the specimen relative to the poles of the magnet. For a magnet of small dimensions,  $C$  changes markedly, even for small changes of specimen position. Before the start of each series of measurements the specimen was placed in the region where  $C$  had its maximum value. Then a displacement of the specimen by  $\pm 0.1$  mm caused the constant  $C$  to diminish by  $\sim 0.5\%$ . By using a photocompensator device, we were able to maintain the specimen position constant with an accuracy of  $\pm 0.03$  mm.

To measure the force  $F$  acting on the specimen, the press 3 was suspended on vertical tungsten wires 6, with a diameter of  $50 \mu$  and length of 10 cm. The lower wire was fixed directly to the press and the upper to plate 7, which was rigidly connected to the press by means of quartz rod 8. The upper end of the upper wire was fixed to the movable stem 9. Rotation of the stem enabled the zero correction of the system to be made, and, by lowering it, it was possible to arrest the balance. Spring 10 maintained a constant tension in the wires. The measurements were made by a compensation method. A compensating moment was created by passing a current through coil 11, which rotated in the gap of permanent horseshoe magnet 12. The current was fed to the coil through the two tungsten wires.

The entire torsional balance was situated in a vacuum jacket, 13, 14, 15, and 16.

An essential part of the apparatus was the press, with the aid of which stresses were created in the specimen. A detailed diagram of the press is given in Fig. 3. Using a suggestion by P. L. Kapitza, the press, suspended on the fine wires, was controlled by a bellows. To bellows 17 were soldered upper and lower rigid plates 18 and 19. After this the bellows was evacuated through capillary 20. The capillary was squeezed off and soldered up. The external atmospheric pressure thus compressed the bellows with a force of  $\sim 2.5$  kg. The lower cap of the bellows lay on supporting frame 21, fixed to the body of the press, 22. On lowering the pressure in the space surrounding the press, elastic forces started to straighten out the compressed bellows. The pressure thus arising was

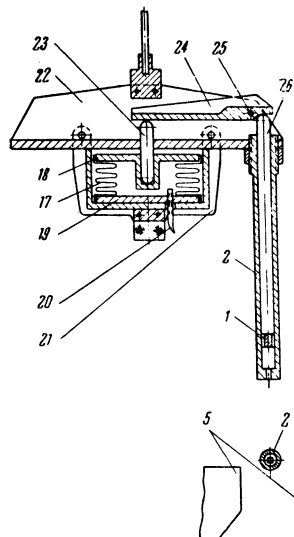


FIG. 3. Diagram of the press and bellows (the numbering of the components follows that of Fig. 2).

transferred through rod 23 to the long arm of lever 24, oscillating about shaft 25, which was fixed to the body of the press. The other lever arm (the ratio of the arms was 1:6) bore on rod 26, by means of which the pressure was transmitted to the specimen, 1. The specimen was at the end of tube 2, screwed into the body of the press. The dependence of the pressure created in the press on the pressure of the helium gas surrounding the press was determined with a wire strain gauge fixed to the side surface of the tube and previously calibrated by using a direct load on rod 26. This dependence was not completely linear, owing to the non-linearity of the bellows compression and small deformations of the lever. Thus, the maximum force acting on the specimen ( $\sim 7$  kg) was smaller than calculated.

The magnetic balance had a photocompensator (used also in our previous work), which automatically maintained the current through compensating coil 11, such that an optical beam reflected from a mirror fixed to plate 7 remained in the null position (with a displacement accuracy dictated by the photocompensator control circuit). In the photocompensator amplifier a differentiating circuit was included which ensured damping of the magnetic balance.\*

The parameters of the compensating system were such that a moment of 1 dyne-cm was created by a current of  $830 \mu\text{a}$ . The uncertainty of the balance reading was approximately  $\pm 0.3 \mu\text{a}$ . The sensitivity can thus be estimated at  $4 \times 10^{-4}$  dyne-cm. For a specimen of weight 10 mg this

\*The author is very grateful to V. I. Ozhogin for constructing the photocompensator circuit, and also to A. N. Vetchinkin for a number of valuable discussions on the choice of the photocompensator circuit.

gave a sensitivity in measuring the susceptibility of  $\sim 2 \times 10^{-6}$  emu/g for  $H = 400$  oe, which is equivalent to a sensitivity in measuring the magnetic moment in the same field of  $\sim 10^{-3}$  emu/g. However, the calibration of the absolute reading was not better than 5%.

All measurements of the piezomagnetic effect were performed at the temperature of liquid hydrogen ( $T = 20.4^\circ \text{K}$ ).

Single crystals of  $\text{MnF}_2$  and  $\text{CoF}_2$  were used; they were grown by N. N. Mikhaïlov and O. S. Zaitsev from a melt subjected to an atmosphere of HF vapor. Small pieces of the crystals, of arbitrary shape and dimensions ( $0.3 \text{ cm}^3$ ), were oriented in the necessary way by an x-ray goniometer. They were then ground by hand to produce a rectangular parallelepiped of dimensions  $1 \times 1 \times 2$  mm. The end of this parallelepiped was glued to the lower end of the rod with BF-2 glue. Then the rod was held in a special mandrel, and the other end of the specimen was ground strictly perpendicular to the axis of the rod. A small layer of vacuum grease ensured a close contact between the specimen and the end of the tube. On applying a pressure  $p$  to the specimen thus mounted, homogeneous stresses arose in it: a)  $\sigma_{ij} = p$  ( $\sigma_{kk} = \sigma_{ll} = \sigma_{ik} = \sigma_{il} = \sigma_{kl} = 0$ ), if the  $i$  axis was along the long edge of the specimen, and b)  $\sigma_{ik} = p/2$  ( $\sigma_{ii} = \sigma_{kk} = p/2$ ,  $\sigma_{ll} = \sigma_{il} = \sigma_{kl} = 0$ ), if the  $i$  and  $k$  axes made angles of  $45^\circ$  with the long edge of the specimen (see Fig. 4).

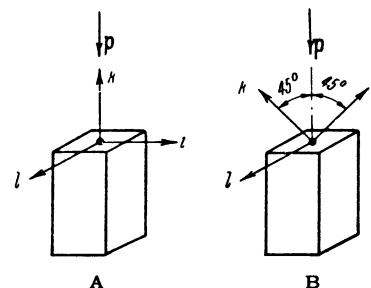


FIG. 4. Orientation of the specimens for investigations on piezomagnetism: A — shear stresses absent, B — a shear stress  $\sigma_{ik} = p/2$  arises.

### 3. RESULTS

The main measurements were made with a  $\text{CoF}_2$  crystal in which the axes were directed as follows:  $i \rightarrow x$ ,  $k \rightarrow z$ ,  $l \rightarrow y$  (see Fig. 4, B). In this case the magnetic field was along the  $y$  axis. Figure 5 shows the variation of magnetic moment  $m_y$  with field, on changing the field within the limits of  $-1.1$  koe to  $+1.1$  koe at liquid-hydrogen temperature ( $T = 20.4^\circ \text{K}$ ). The line 1 was obtained when no pressure was applied to the specimen. The experimental results in this case are described by the equation

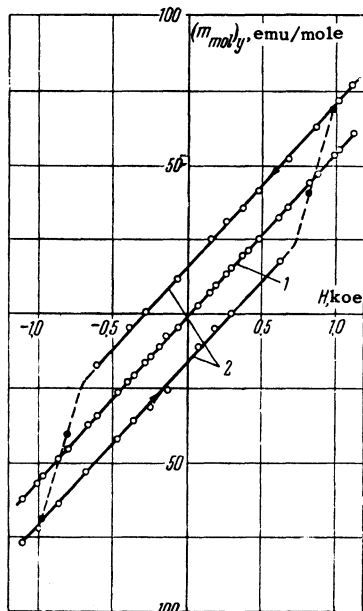


FIG. 5. Variation of molar magnetic moment  $m_y$  of  $\text{CoF}_2$  with magnetic field: 1 - in the absence of stress, 2 - under a stress  $\sigma_{xz} = 340 \text{ kg/cm}^2$ .

$$m_y = m_y^0 + \chi_y^0 H,$$

where  $\chi_y^0 = 56 \times 10^{-3} \text{ emu/mole}$  and  $m_y^0 = -1 \text{ emu/mole}$ . On applying to this specimen the maximum pressure obtained,  $p = 680 \text{ kg/cm}^2$ , the experimental points are described by two straight lines (2 in Fig. 5)

$$m_y = \pm m_y^p + \chi_y^p H. \quad (2)$$

The value of the spontaneous moment  $m_y^p = 16 \text{ emu/mole}$  and does not depend on the field. In weak fields (up to 500 oe) the direction of the moment remains unchanged. For large fields in the opposite direction to the moment  $m_y^p$ , the magnetization of the specimen reverses. The reversal of magnetization takes place comparatively slowly. For a field of 810 oe,  $\sim 40\%$  reversal of magnetization occurs in 5 minutes. Further change is very slow. On increasing the field further to 980 oe, almost complete reversal of magnetization takes place in 7 minutes. The results on magnetization reversal were not well reproducible; we have therefore limited ourselves to a qualitative study, and in Fig. 5 the region of magnetization reversal is tentatively shown by broken lines.

The results obtained in Fig. 5, and additional measurements at two intermediate pressures, show that within the limits of accuracy of our experiments the paramagnetic susceptibility  $\chi_y$  does not change on applying pressure. Therefore, we studied the variation of piezomagnetic moment  $m_y^p$  on pressure by measuring the change of the total moment  $m_y$  in a constant magnetic field,  $H = 1.1 \text{ koe}$ , while changing the pressure on the specimen. The results of these measurements

are given in Fig. 6, from which it is seen that  $m_y^p$  varies linearly with pressure, with

$$m_y^p = 5.1 \cdot 10^{-2} \sigma_{xz} \text{ emu/mole} = 2.1 \cdot 10^{-3} \sigma_{xz} \text{ gauss} \quad (\sigma_{xz} \text{ in kg/cm}^2).$$

Measurements were made on the same crystal of the magnetic moment along the [101] direction,

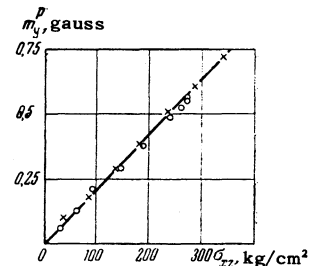


FIG. 6. Variation of transverse piezomagnetic moment per unit volume  $m_y^p$  for  $\text{CoF}_2$  on the value of the applied shear stress  $\sigma_{xz}$ .

where the field was perpendicular to the y axis. As in the previous case, a small residual moment  $m^0 = 1.1 \text{ emu/mole}$  was observed. On applying pressure its value changed only by 30%.

Analogous results were obtained on a specimen in which the axes were directed as follows:  $i \rightarrow x$ ,  $k \rightarrow y$ ,  $l \rightarrow z$ . During measurements of the magnetic moment  $m_z$  (the field H was along the z axis), curves were obtained analogous to those shown in Fig. 5. In this case

$$\chi_z^0 = \chi_z^p = 13 \cdot 10^{-3} \text{ emu/mole}, \quad m_z^0 = 1.2 \text{ emu/mole}.$$

On applying pressure a piezomagnetic moment  $m_z^p$  appears, which also varies linearly with pressure (Fig. 7):

$$m_z^p = 1.9 \cdot 10^{-2} \sigma_{xy} \text{ emu/mole} = 0.8 \cdot 10^{-3} \sigma_{xy} \text{ gauss} \quad (\sigma_{xy} \text{ in kg/cm}^2).$$

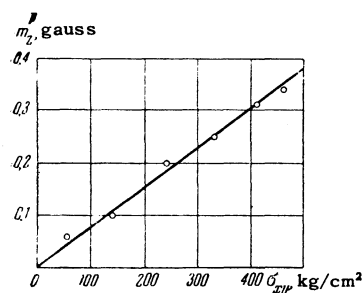


FIG. 7. Variation of the longitudinal piezomagnetic moment per unit volume  $m_z^p$  for  $\text{CoF}_2$  on the value of the applied shear stress  $\sigma_{xy}$ .

During magnetic measurements along the [110] axis we also observed a small residual moment,  $m^0 = 0.8 \text{ emu/mole}$  which changed by 30% on applying the maximum pressure.

A specimen was also studied with axes oriented as shown in Fig. 4,A ( $i \rightarrow x$ ,  $k \rightarrow y$ ,  $l \rightarrow z$ ). In this specimen also, residual moments  $m_x^0 = 1 \text{ emu/mole}$ ,  $m_z^0 = 1.3 \text{ emu/mole}$  were observed, which changed on applying the maximum pressure by 30 and 20%.

A piezomagnetic effect was also discovered in the  $\text{MnF}_2$  crystal. The results shown in Fig. 8

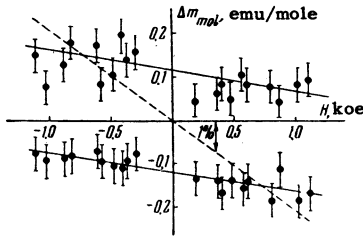


FIG. 8. The piezomagnetic effect in  $\text{MnF}_2$ . The broken curve corresponds to a susceptibility change of 1%.

were obtained on a specimen having the orientation shown in Fig. 4, B ( $i \rightarrow x$ ,  $k \rightarrow z$ ,  $l \rightarrow y$ , the field  $H$  applied along the  $y$  axis). Because the piezomagnetic moment amounted to only  $\sim 1\%$  of the paramagnetic moment  $\chi H$ , on the abscissa axis is plotted the difference of moments measured under pressure ( $p = 520 \text{ kg/cm}^2$ ), and without pressure,  $\Delta m = m_y^p - m_y^0$ . The results obtained show that under a pressure  $p = 520 \text{ kg/cm}^2$ , a piezomagnetic moment  $m_y^p = 0.12 \text{ emu/mole} = 5 \times 10^{-3} \text{ gauss}$  appears in the specimen. Together with this slight ( $\sim 0.2\%$ ) decrease in the susceptibility occurs. We found that the direction of the piezomagnetic moment remains unchanged on applying a field in the opposite direction of a magnitude up to the maximum we used  $-1.1 \text{ koe}$ . The direction of the piezomagnetic moment could only be changed if the compressed specimen was cooled in the magnetic field from a temperature above the Néel point ( $T_N = 67.5^\circ \text{K}$ ) to hydrogen temperature. The direction of the piezomagnetic moment was always coincided with the direction of the field in which the specimen was cooled. This direction was then always preserved during repeated pressure removals and applications of opposing fields. Thus, depending on the direction of the field in which the compressed specimen was cooled, we obtain the points which belong to the upper and lower lines in Fig. 8.

#### 4. DISCUSSION OF RESULTS

1) Following Dzyaloshinskii,<sup>5,12</sup> the thermodynamic potential for the investigated fluorides, taking into account relativistic terms linear in the stress  $\sigma_{ijk}$  and in the magnetic moment  $\mathbf{m} = \mathbf{s}_1 + \mathbf{s}_2$ , and invariant with respect to transformations of the group  $D_{4h}^{14}$ , can be written in the following form:

$$\begin{aligned} \tilde{\Phi} = & \frac{1}{2} a (\gamma_x^2 + \gamma_y^2) + \frac{1}{2} B m^2 + \frac{1}{2} b m_z^2 + e (\gamma_x m_y + \gamma_y m_x) \\ & + \lambda_1 (m_x \sigma_{yz} + m_y \sigma_{xz}) \gamma_z + \eta_1 (\gamma_y \sigma_{yz} + \gamma_x \sigma_{xz}) \gamma_z \\ & + \lambda_2 m_z \gamma_z \sigma_{xy} + \eta_2 \gamma_x \gamma_y \sigma_{xy} - mH, \end{aligned} \quad (3)$$

where  $\gamma_x$ ,  $\gamma_y$ ,  $\gamma_z$  are the components of a unit

vector along the antiferromagnetic vector  $\mathbf{l} = \mathbf{s}_1 - \mathbf{s}_2$ . As is seen from Fig. 1, in the absence of an external field and stresses ( $H = 0$  and  $\sigma_{ijk} = 0$ )  $\gamma_x = \gamma_y = 0$ . To this corresponds the condition  $a' = a - e^2/B > 0$ .

We shall use polar coordinates  $\theta$  and  $\varphi$  to label the directions of the vector  $\gamma$ . Analysis of the thermodynamic potential (3) in the absence of stresses shows that on applying an external field  $H$ , the angle  $\theta$  remains equal to zero if the field is along the  $z$  axis. If the field has a component  $H_\perp$  perpendicular to the  $z$  axis, the appearance of a magnetization  $\mathbf{m}_\perp = (a/a'B) H_\perp$  is accompanied by a rotation of  $\mathbf{l}$  by an angle  $\theta = eH_\perp/a'B$ . Here the condition  $\psi + \varphi = \pi/2$  should be satisfied ( $\psi$  is the angle between  $H_\perp$  and the  $x$  axis).

We shall analyze the thermodynamic potential (3) in the presence of elastic stresses for the particular cases occurring in our experiments.

2) For the first specimen we have  $\sigma_{xy} = \sigma_{yz} = 0$ ,  $\sigma_{xz} \neq 0$ . In this case minimization of the potential in the absence of a field gives\*

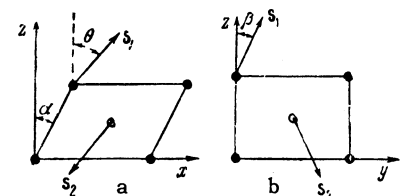
$$\theta = |\sigma_{xz}| (\eta_1 B - e \lambda_1) / (aB - e^2) \quad (4a)$$

and  $\varphi = 0$  or  $\pi$  depending on the sign of  $\sigma_{xz}$ . Thus, in agreement with the result obtained by Dzyaloshinskii,<sup>5</sup> a spontaneous moment arises along the  $y$  axis:

$$m_y^p = \sigma_{xz} (e \eta_1 - a \lambda_1) / (aB - e^2). \quad (4b)$$

In this way the application of a stress  $\sigma_{xz}$  causes, as is shown schematically in Fig. 9, the magnetization of the sublattices to be no longer strictly antiparallel, and by rotating in the  $zy$  plane they include an angle  $\pi - 2\beta$ , where  $\beta = m_y^p/l$ . This is

FIG. 9. Rotations of the magnetic moments of the sublattices in the transverse piezomagnetic effect: a - in the  $xz$  plane, and b - in the  $yz$  plane.



accompanied by the rotation of the antiferromagnetic vector as a whole through an angle  $\theta$  in the  $xz$  plane. This picture agrees completely with what was observed in previously studied antiferromagnets with weak transverse ferromagnetism.

The application of a magnetic field along the  $y$  axis increases the angle  $\theta$  by  $eH_y/a'B$ ; the following expression is obtained for the magnetic

\*In all the calculations which follow we assume that in the initial state  $\theta_0 = 0$ . If we take the initial value  $\theta_0 = \pi$ , then the expression for  $\theta'$  will have the form  $\theta' = \pi - \theta$ ; piezomagnetic moments change sign on inversion.

moment in this case:

$$m_y = m_y^p + (a/a'B)H_y. \quad (5)$$

This conclusion of the theory is in complete agreement with what we observed in experiment [see Fig. 5 and Eq. (2)]. The experimental data we obtained allow the evaluation of the rotation angle of the sublattices and some of the coefficients of the expression. For further calculation we will neglect the difference between  $a$  and  $a'$  (taking  $e^2/B \ll a$ ). Then, in the case of  $\text{CoF}_2^*$  we have  $B = 1/\chi_{\perp} = 0.5 \times 10^3$ ; assuming that both terms in (4b) give approximately equal contributions, we obtain an estimate for the coefficient  $\lambda_1 \sim 0.5$  (in any case  $\lambda_1 \leq 1$ ). On applying the stress  $\sigma_{xz} = 500 \text{ kg/cm}^2$ , we obtain the following estimates for the angles:  $\alpha = \sigma_{xz}/G \sim 2 \times 10^{-3}$  (the shear modulus  $G$  was here taken to be  $0.25 \times 10^{-6} \text{ kg/cm}^2$ );  $\beta = m_y^p/l \sim 5 \times 10^{-3}$ . To evaluate  $\theta$  it does not suffice to know the coefficients  $e$  and  $a$ . If it is assumed that the value of the relativistic terms amounts to  $\sim 10^{-3}$  of the exchange energy, then for the angle  $\theta$  the value  $\sim 10^{-3}$  is obtained, i.e., all three angles are of the same order of magnitude.

If the applied field is directed perpendicular to the  $y$  axis, minimization of the potential (3) gives the following solution for the components of the moment:

$$m_x = (a/a'B)H_x, \quad m_y = m_y^p, \quad m_z = H_z/(B + b),$$

which also agrees with our measurements of the moments along the  $[101]$  axis — in this direction the magnetic properties do not depend on pressure and the crystal does not display ferromagnetism (we shall return to the weak parasitic moment). The angle  $\theta$  is changed by the field also, as in the previous case, whilst the angle  $\varphi$  does not remain constant, but increases gradually and tends in large fields ( $eH_x \gg B\eta_1\sigma_{xz}$ ) to  $\varphi = \pi/2$ .

3) Special interest attaches to the case  $\sigma_{xz} = \sigma_{yz} = 0$ ;  $\sigma_{xz} \neq 0$ . In this case, in the absence of a field, the direction of the spontaneous magnetization vector is not changed on applying pressure ( $\theta = 0$ ). A piezomagnetic moment, as already shown,<sup>12</sup> is obtained along the  $z$  axis:

$$m_z^p = \lambda_2\sigma_{xy}/(B + b).$$

Thus there arises here weak longitudinal ferromagnetism, which has not been previously observed. In distinction from the transverse, the longitudinal weak ferromagnetism is caused by

\*Below all quantities are given in the cgs emu system calculated for  $1 \text{ cm}^3$  of substance. The pressures are given in  $\text{kg/cm}^2$ .

the difference in the values of the magnetic moments of the ions in the two sublattices. As is seen from Fig. 10, the ions 1 and 2, which are equivalent before deformation with respect to symmetry of the crystalline field, after shear deformation in the  $xy$  plane, cease to be equivalent. It is apparent that, if the change of the angle between the  $x$  and  $y$  axes from  $\pi/2$  causes such a change of the crystalline field, while the size of the magnetic moments changes linearly with deformation, then the signs of these changes in both sublattices should be opposite. The microscopic nature of the different changes of the crystalline fields for different ions is connected with the different signs of the changes in distance to nearest fluoride ions, as seen from Fig. 10.

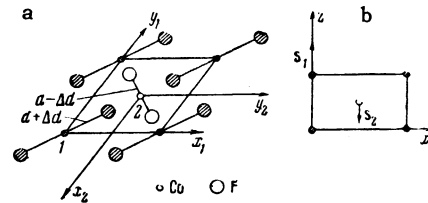


FIG. 10. The longitudinal piezomagnetic effect: a — the change of symmetry of the crystalline fields, b — the change of the sublattice magnetic moments.

On applying a magnetic field the angles  $\varphi$  and  $\theta$  change, to a first approximation, just as they do in the undeformed crystal, and for the magnetic moments the solution is obtained

$$m_{\perp} = (a/a'B)H_{\perp}, \\ m_z = H_z/(B + b) + \lambda_2\sigma_{xy}/(B + b). \quad (6)$$

This result also agrees completely with what we observed in the experiments with the second  $\text{CoF}_2$  specimen. From the experimental data the value  $\lambda_2 = 1.6$  is found directly.

4) The crystallographic symmetry of the fluorides is such that the thermodynamic potential only contains terms for shear stresses  $\sigma_{ik}$  ( $i \neq k$ ). This agrees with the negative results obtained on the third  $\text{CoF}_2$  crystal, where we provided only compressive stresses ( $\sigma_{ij}$ ).

5) During measurements on all the specimens we encountered a weak ferromagnetic moment even in undeformed crystals. The size of this moment varied within limits of up to  $1\frac{1}{2}$  times in different specimens, and was approximately 10 times smaller than the piezomagnetic moments we observed. In distinction from the latter, this moment was practically isotropic. The size of the observed parasitic moment was such that it could be caused by a susceptibility decrease of  $\sim 2\%$  on changing from a field of 1 koe to a field of 10 koe.

It should be pointed out that a variation of  $\chi$  on H in  $\text{CoF}_2$  of such an order has also been observed by other workers.<sup>19,20</sup> It is possible that the parasitic moment is caused by a piezomagnetic effect due to inhomogeneous internal stresses in the specimens studied. However, an anneal we carried out on one of the specimens did not change the value of the moment.

6) The thermodynamic theory naturally cannot predict the size of the piezomagnetic effect. Dzyaloshinskiĭ,<sup>18</sup> from very crude premises, has given a formula to estimate the size of the piezomagnetic modulus:

$$\Lambda \sim \sqrt{a\chi/\Theta E},$$

where  $\Theta$  is the Néel temperature in energy units and  $E$  is Young's modulus. The ratio  $a/\Theta$ , according to the data on the weak ferromagnetism, lies within the limits  $10^{-2}$  and  $10^{-5}$ . Accordingly, an estimate for  $\Lambda$  gives a value of  $10^{-3}$  to  $10^{-4}$ . The result for  $\text{MnF}_2$  gave a value an order smaller than the lower limit of this estimate, which is not unreasonable, considering the crudity of the estimate. The smallness of the piezomagnetic effect in  $\text{MnF}_2$  is easily explained if it is assumed that the weak ferromagnetism is caused by spin-orbital and not dipole interactions.\* For the  $\text{Mn}^{++}$  ion in the S state, the spin-orbital interaction should be very small. Most favorable in this respect is the  $\text{Co}^{++}$  ion. The particular splitting of its ground state by the crystalline field<sup>22,23</sup> means that the effect of spin-orbital interaction in it should be the greatest of all the transition element ions. With this is apparently associated the anomalously large size of the piezomagnetic effect. In particular this refers to the longitudinal effect, which is entirely due to the effect of the crystalline fields.

7) From the thermodynamic discussion given above, it follows that for the same sign of  $\sigma_{ik}$  the direction of the piezomagnetic moment is uniquely connected with the direction of the antiferromagnetic vector ( $m_Y^D \sim \sin \theta$ ;  $m_Z^D \sim \cos \theta$ , where the angle  $\theta$  lies within the limits 0 and  $\pi$ ). Therefore, a reversal of the piezomagnetic moment by an external field should be accompanied by a rotation of the antiferromagnetic vector  $l$  through  $180^\circ$ . The two states with  $\theta = 0$  and  $\theta = \pi$  are divided by a potential barrier with a height of the order of the anisotropy energy  $a \sim 10^7$  erg/cm<sup>3</sup>. In our experiments we showed that in the same crystal repeatedly cooled, the

\*This has been shown for rhombohedral structures by Bertaut;<sup>21</sup> analogous calculations confirm this effect for the fluorides also.

spontaneous moment observed in the absence of a field was always in the same direction. This indicates two facts: a) in the crystals studied a single-domain antiferromagnetic structure is formed, b) the direction of the antiferromagnetic vector in a given crystal is always the same, for which some imperfection of the crystal is responsible, causing the energetic preference of one of the states. The energy difference can be estimated from the size of the magnetic energy required for magnetization reversal. In our experiments magnetization reversal was observed for  $mH \sim 5 \times 10^2$  erg/cm<sup>3</sup>. We established that this value decreased somewhat (by  $\sim 30\%$ ) after an anneal of one of the specimens. It should be emphasized that the energy indicated is four orders smaller than the height of the potential barrier. It can be assumed, therefore, that the observed magnetization reversal time (in our experiments  $\tau \sim 30$  sec) is associated with the lifetime of the sublattices. However, to obtain quantitative conclusions, it is necessary to develop the theory of magnetization reversal kinetics, and perform further experiments in this area.

8) In view of the low accuracy in orienting the crystals, the values we obtained for  $\chi_\perp$  and  $\chi_\parallel$  at  $T = 20.4^\circ\text{K}$  can contain significant errors — up to 10% of the difference  $\chi_\perp - \chi_\parallel$ . Up to the present only the difference of susceptibilities<sup>19</sup> has been measured in  $\text{CoF}_2$  single crystals. Our data,  $\chi_\perp - \chi_\parallel = 43 \times 10^{-3}$  emu/mole, agree within the limits of accuracy indicated above, with the value  $48 \times 10^{-3}$  emu/mole obtained by Stout and Mataresse.<sup>19</sup> In this connection, attention should be turned to the fact that in the case of  $\text{CoF}_2$  the susceptibility  $\chi_\parallel$  does not apparently tend to zero as  $T \rightarrow 0^\circ\text{K}$ .

In conclusion, the author expresses his deep gratitude to Acad. P. L. Kapitza for constant interest in the work, N. N. Mikhaĭlov and O. S. Zaitsev for making the  $\text{MnF}_2$  and  $\text{CoF}_2$  single crystals, I. E. Dzyaloshinskiĭ for useful discussions, and also V. I. Kolokol'nikov for assistance in carrying out the experiments.

Note added in proof (March 9, 1960). Moriya, in a recently published paper [T. Moriya, J. Phys. Chem. Solids **11**, 73 (1959)], by considering the change of potential of the crystalline field during compression in the [110] direction, evaluated the quantity  $\Lambda_2 = 4 \times 10^{-3}$  gauss/(kg/cm<sup>2</sup>), which is only eight times greater than our experimental result.

<sup>1</sup>W. Voigt, Lehrbuch der Kristallphysik, Leipzig (1928).

- <sup>2</sup> L. D. Landau and E. M. Lifshitz, *Статистическая физика (Statistical Physics)*, GITTL, (1951).
- <sup>3</sup> B. A. Tavger and V. M. Zaitsev, *JETP* **30**, 564 (1956), *Soviet Phys. JETP* **3**, 430 (1956).
- <sup>4</sup> L. D. Landau and E. M. Lifshitz, *Электродинамика сплошных сред (Electrodynamics of Continuous Media)*, Gostekhizdat (1957).
- <sup>5</sup> I. E. Dzyaloshinskiĭ, *JETP* **33**, 807 (1957), *Soviet Phys. JETP* **6**, 621 (1958).
- <sup>6</sup> B. A. Tavger, *Кристаллография* **3**, 342 (1958), *Soviet Phys.-Crystallography* **3**, 344 (1959).
- <sup>7</sup> Y. Le Corre, *J. phys. radium* **19**, 750 (1958).
- <sup>8</sup> L. Néel and R. Pauthenet, *Compt. rend.* **234**, 2172 (1952). L. Néel, *Revs. Modern Phys.* **25**, 58 (1953).
- <sup>9</sup> A. S. Borovik-Romanov and M. P. Orlova, *JETP* **31**, 579 (1956), *Soviet Phys. JETP* **4**, 531 (1957).
- <sup>10</sup> A. S. Borovik-Romanov, *JETP* **36**, 766 (1959), *Soviet Phys. JETP* **9**, 539 (1959).
- <sup>11</sup> I. E. Dzyaloshinskiĭ, *JETP* **32**, 1547 (1957), *Soviet Phys. JETP* **5**, 1259 (1957).
- <sup>12</sup> I. E. Dzyaloshinskiĭ, *JETP* **33**, 1454 (1957), *Soviet Phys. JETP* **6**, 1120 (1958).
- <sup>13</sup> A. S. Borovik-Romanov, *JETP* **36**, 1954 (1959), *Soviet Phys. JETP* **9**, 1391 (1959).
- <sup>14</sup> J. W. Stout and H. E. Adams, *J. Amer. Chem. Soc.* **64**, 1535 (1942).
- <sup>15</sup> J. W. Stout and E. Catalano, *Phys. Rev.* **92**, 1575 (1953).
- <sup>16</sup> R. W. G. Wyckoff, *The Structure of Crystals*, N.Y. (1931).
- <sup>17</sup> R. A. Erickson, *Phys. Rev.* **90**, 779 (1953).
- <sup>18</sup> I. E. Dzyaloshinskiĭ, *Dissertation*, Moscow (1957).
- <sup>19</sup> J. W. Stout and L. M. Mataresse, *Revs. Modern Phys.* **25**, 338 (1953).
- <sup>20</sup> W. J. de Haas and B. H. Schultz, *Physica* **6**, 481 (1939).
- <sup>21</sup> F. Bertaut, *Compt. rend.* **246**, 3335 (1958).
- <sup>22</sup> A. Abragam and M. H. L. Pryce, *Proc. Roy. Soc. A* **206**, 173 (1951).
- <sup>23</sup> T. Nakamura and H. Taketa, *Progr. Theor. Phys.* **13**, 129 (1955).

Translated by K. F. Hulme  
217